Equatorward diffuse auroral emissions at Jupiter: Simultaneous HST and Galileo observations

A. Radioti,[1] A. T. Tomás,[2] D. Grodent,[1] J.-C. Gérard,[1] J. Gustin,[1] B. Bonford,[1] N. Krupp,[3] J. Woch,[3] and J. D. Menietti[4]

Received 26 February 2009; accepted 4 March 2009; published 2 April 2009.

[1] We study the auroral emissions equatorward of the main oval based on Hubble Space Telescope (HST) observations of both Jovian hemispheres on September 20, 1997. On the same day, Galileo observed changes in the electron pitch angle distribution between the inner and middle magnetosphere (PAD boundary), indicative of electron diffusion. This region, magnetically maps to the equatorward diffuse emissions on both hemispheres. Whistler mode waves, observed simultaneously, can scatter electrons into the loss cone and lead to electron precipitation in the ionosphere. Based on simultaneous HST FUV and Galileo wave and electron data we test the conditions for electron scattering by whistler mode waves and derive the energy flux precipitated in the ionosphere. The comparison of the derived precipitation energy flux with the observed auroral brightness indicates that the energy contained in the PAD boundary can account for the auroral emissions.
Citation: Radioti, A., A. T. Tomás, D. Grodent, J.-C. Gérard, J. Gustin, B. Bonfond, N. Krupp, J. Woch, and J. D. Menietti (2009), Equatorward diffuse auroral emissions at Jupiter: Simultaneous HST and Galileo observations, *Geophys. Res. Lett.*, *36*, L07101, doi:10.1029/2009GL037857.

1. Introduction

[2] Analysis of Hubble Space Telescope (HST) ultraviolet images has shown that Jupiter's auroral emissions are divided into three main components characterised by their locations, the physical processes from which they originate, and their time variations [*Clarke et al.*, 1998; *Grodent et al.*, 2003a, 2003b]. With increasing latitude these three components are: the satellite footprints, the main emission or main oval and the polar emissions. A fourth component can be defined by the auroral emissions located equatorward of the main oval and poleward of the Io footprint, the equatorward diffuse emissions (EDE). They consist of emissions extending from the main oval towards lower latitudes, occasionally forming discrete belt of emissions parallel to the main oval [*Grodent et al.*, 2003a] and/or patchy irregular emissions. The morphology and brightness of the main oval have been extensively examined the last years [i.e., *Grodent et al.*, 2003a] and theoretical approaches associated the emissions with the ionosphere-magnetosphere coupling current system related to the breakdown of corotation in the middle magnetosphere [i.e., *Cowley and Bunce*, 2001]. However, only a few studies were focused on the morphology and origin of the diffuse emissions equatorward of the main oval.

[3] In the magnetosphere of the Earth the origin of the diffuse auroral electron precipitation is mainly discussed in terms of precipitation by electrostatic electron cyclotron harmonic and whistler mode waves [i.e., *Horne et al.*, 2003]. At Jupiter, *Bhattacharya et al.* [2001] suggested that wave particle interactions in a broad region in the magnetosphere (10 to 25 R_J) could lead to electron scattering and precipitation into the ionosphere contributing to the EDE. *Tomás et al.* [2004b] related the transition of the electron pitch angle distribution (PAD) from pancake to bidirectional (observed within 10 to 17 R_J) to a discrete auroral emission equatorward of the main oval, under the assumption of electron scattering due to whistler mode waves. A similar PAD evolution and electron scattering by whistler waves was observed closer to the planet at $\sim$6 R_J and was associated with an interchange event [*Xiao et al.*, 2003]. Additionally, sporadic energetic electron injection events were related to transient isolated auroral patches equatorward of the main oval [*Mauk et al.*, 2002; *Bhattacharya et al.*, 2005]. In the present work we aim to study the origin of the EDE at both hemispheres and their relation to electron scattering by whistler mode waves based on a unique set of simultaneous HST and Galileo observations.

2. Simultaneous HST and Galileo Observations

[4] Figure 1 shows auroral polar projections of the northern and southern Jovian hemisphere in a reference frame fixed to the Sun, with the Sun to the bottom and dusk to the right. The images were taken by the HST/STIS (Space Telescope Imaging Spectrograph) camera 1.5 hour apart on September 20, 1997. The main auroral features, i.e., the main oval, the Io footprint and the polar emissions are indicated for both hemispheres. In order to define the boundaries of the EDE, the main oval should be identified. The main oval is restricted to a short arc in the morning sector, followed by a discontinuity close to noon [*Radioti et al.*, 2008], while in the afternoon sector the emission shows a less structured arc [*Grodent et al.*, 2008a]. In the northern hemisphere there is a distortion of the main emission shape, in the "kink sector" (80°–150° in S3 coordinate system, here in the afternoon local time sector). It could result from a magnetic field anomaly in the north pole [*Grodent et al.*, 2008b]. The dashed line contour in Figure 1 defines a region of broad diffuse emissions, equatorward of the main emission in the dusk side at both hemispheres. The emission follows the

[1] Laboratoire de Physique Atmosphérique et Planétaire, Institut d'Astrophysique et de Géophysique, Université de Liège, Liège, Belgium.
[2] GeoForschungsZentrum, Potsdam, Germany.
[3] Max-Planck-Institut für Sonnensystemforschung, Katlenburg-Lindau, Germany.
[4] Department of Physics and Astronomy, University of Iowa, Iowa City, Iowa, USA.

0094-8276/09/2009GL037857$05.00

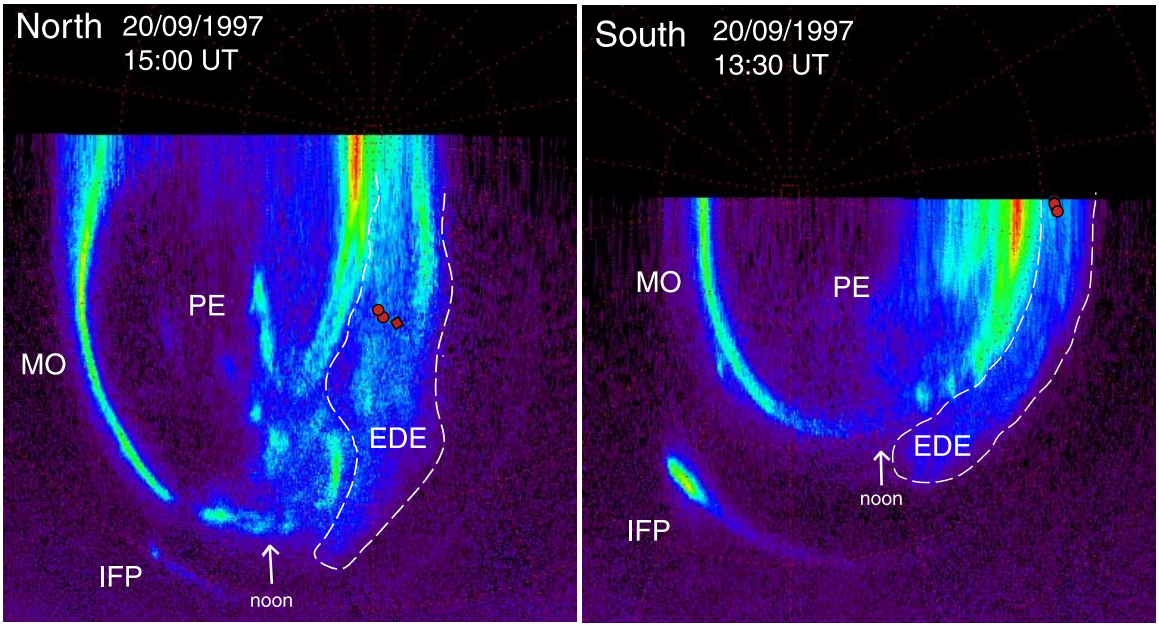

Figure 1. Polar projections of HST STIS images in a reference frame fixed to the sun, with the sun to the bottom and dusk to the right. The images show the northern and southern Jovian aurora on September 20, 1997 at 15:00 UT and at 13:30 UT, respectively. The arrow indicates the magnetic noon. The main auroral features are shown: the main oval (MO), the Io footprint (IFP) and its trail and the polar emissions (PE). The dashed line contour defines the region of equatorward diffuse emissions (EDE) in the dusk side. The red dots indicate the mapped location of the pitch angle distribution boundary observed by Galileo in the equatorial plane on the same day at 01:00–03:00 UT, using a magnetic field model accounting for the magnetic anomaly [*Grodent et al.*, 2008b] for the northern hemisphere and the VIP4 magnetic field model [*Connerney et al.*, 1998] for the southern hemisphere. The red diamond in the northern polar projection shows Ganymede's observed footprint, when Ganymede's equatorial position is at 40 S3 longitude [*Grodent et al.*, 2008b, Table 1].

structure of two quasi-parallel arcs, which are more prominent in the north than in the south. The observed brightness in the EDE region above the background emission is corrected for the limb brightening effect (geometric accumulation of light along the line of sight when approaching the limb) using $\cos\theta$ factor, where θ is the zenithal angle. It ranges from 40 to 100 kR in the north and from 10 to 50 kR in the south and it considers H_2 emission plus Lyman-a [*Grodent et al.*, 2001]. Based on the analysis of the large HST 1997–2007 dataset we note that the EDE are almost always present, especially in the dusk side, confirming previous observations [*Grodent et al.*, 2003a]. The persistence of the EDE allows us to compare them with Galileo data taken several hours before.

[5] On the same day the HST data was taken, Galileo was in the dusk side of the Jovian magnetosphere between 10 and 20 R_J. Figure 2a shows an equatorial projection of the Galileo orbit, between September 18 and 22, 1997. Figure 2b depicts the normalised PAD of the 29–42 keV electron channels, measured by Galileo EPD (Energetic Particles Detector), during September, 19 and 20 1997, as a function of time and radial distance. At radial distances smaller than 17 R_J the distribution shows a maximum at 90° (pancake distribution) indicative of a population stably trapped in the magnetic field. Further evidence of a pancake distribution at distances <17 R_J comes from the EPD observations during other Galileo orbits and from the high resolution data whenever they are available [*Tomás et al.*, 2004a]. Beyond 18.5 R_J the distribution is bidirectional, meaning that the electron fluxes are predominately directed parallel or antiparallel to the magnetic field lines. The position of the distinct change in the electron PAD from pancake to bidirectional is called PAD boundary and is observed in most of Galileo orbits [*Tomás et al.*, 2004a]. In the present case the boundary is defined by the solid vertical lines in Figure 2 at ~17–18.5 R_J, based on

Figure 2. (a) Galileo trajectory during September 18–22, 1997 (Doy 261–265, 1997) on the equatorial plane, with Jupiter in the center and the sun to the bottom. Part of the trajectory during which the pitch angle distribution (PAD) is studied is indicated by green and the location of the PAD boundary by red. (b) Normalised PAD of electrons (304–527 keV, Galileo EPD) from 12:00 UT, doy 262 to 12:00 UT, doy 263, within 40 R_J from the planet. The PAD boundary is located between 01:00 UT and 03:00 UT, on September 20, 1997 (doy 263) and is marked by the vertical solid lines. (c) Frequency-time spectrogram depicting the intensity of the electric field component of waves for the time interval under study. (d) E (left) and B (middle) field power spectrum based on wave measurements during the PAD boundary (01:00–03:00 UT). The solid and dashed lines show the maximum and minimum values at a given wave frequency. Galileo EPD electron energy spectra (right) at the energy range of 15 to 304 keV during the same time interval. The spectra corresponds to a minimum (01:40 UT) and maximum (02:48 UT) energy flux.

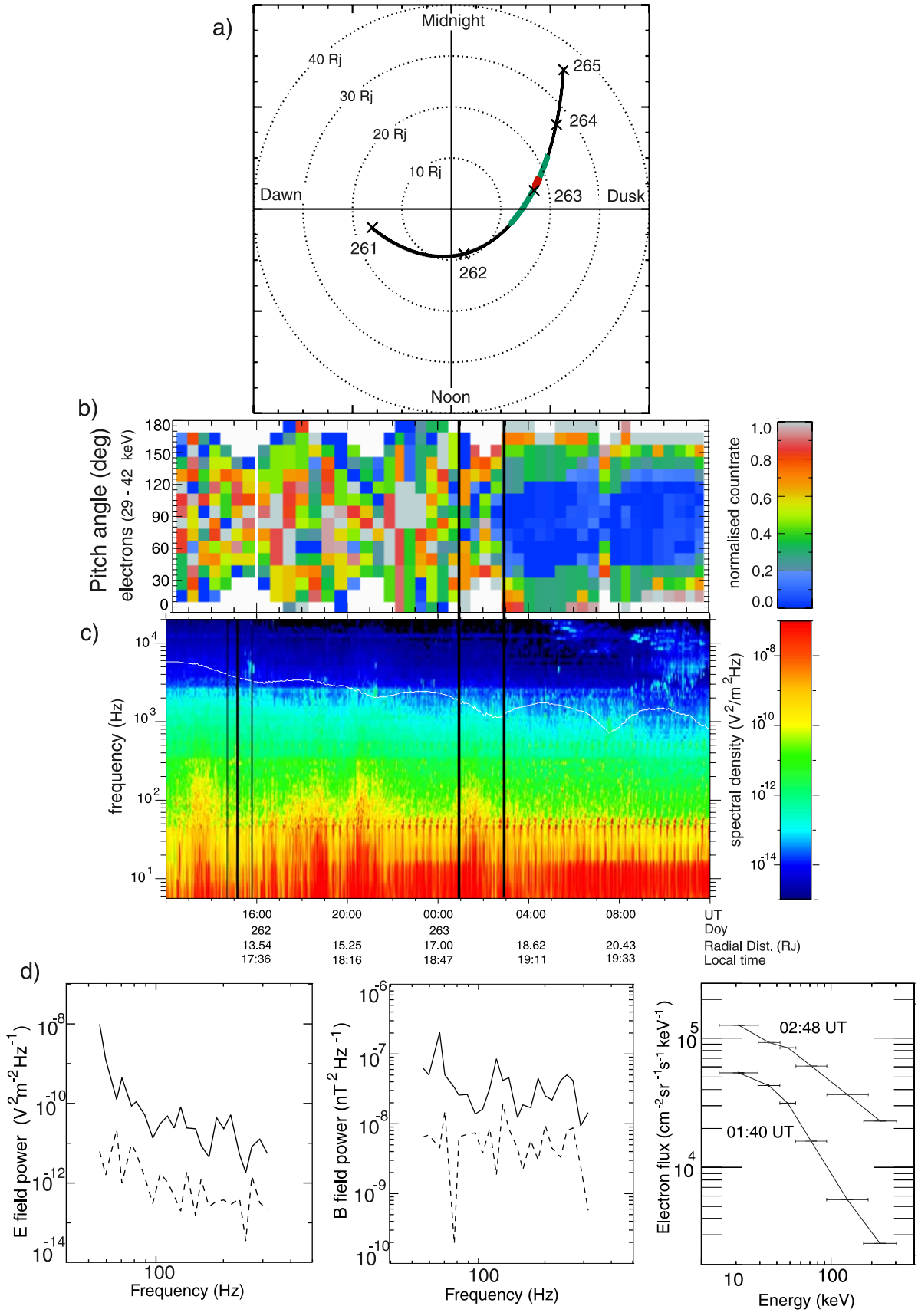
a)
Midnight
40 Rj
30 Rj
20 Rj
10 Rj
Dawn
Dusk
Noon
265
264
263
262
261
b)
Pitch angle (deg)
electrons (29 - 42 keV)
normalised countrate
c)
frequency (Hz)
spectral density (V²/m²Hz)
16:00
20:00
00:00
04:00
08:00
UT
262
263
Doy
13.54
15.25
17.00
18.62
20.43
17:36
18:16
18:47
19:11
19:33
Radial Dist. (RJ)
Local time
d)
E field power (V²m⁻²Hz⁻¹)
B field power (nT²Hz⁻¹)
Frequency (Hz)
Frequency (Hz)
Electron flux (cm⁻²sr⁻¹s⁻¹keV⁻¹)
02:48 UT
01:40 UT
Energy (keV)

Figure 2

measurements at the whole EPD energy range. Figure 2c shows the frequency-time spectrogram of the intensity of the wave electric field component measured by the wave instrument onboard Galileo. The region of the boundary contains a distinct increase in the wave intensity at frequencies from 55 to 300 Hz, indicative of low-frequency whistler mode emission. Emissions at frequencies below 55 Hz are contaminated and are not taken into account in our analysis.

[6] We take advantage of the simultaneous HST and Galileo observations to investigate the relation between the EDE and the PAD boundary. Special care is taken for the magnetic mapping especially in the 'kink' region in the northern hemisphere. Recent studies [*Grodent et al.*, 2008b] showed that VIP4 magnetic field model [*Connerney et al.*, 1998] does not reproduce well the satellite footprints in the region of the magnetic anomaly. Thus, in the present analysis we use the updated model described by *Grodent et al.* [2008b]. This model includes an additional magnetic dipole counterpart in the northern hemisphere, which accounts for the deviation of the satellites' footprints in the 'kink sector'. The red dots on the northern polar projection (Figure 1) indicate the mapped location of the boundary observed by Galileo ~11 hours before the HST image was taken. The boundary maps on the region of the EDE and in particular on the poleward discrete belt of auroral emissions. The measured brightness on the magnetically mapped location of the boundary is ~50 kR. The reliability of the magnetic mapping is further increased by a model free method, which takes advantage of the fact that the satellite footprints are magnetically connected to the moons and serve as absolute reference points for the magnetic mapping from the equatorial plane to the ionosphere. On top of the aurora image (Figure 1) we overplot with the red diamond the location of Ganymede's footprint, when the S3 orbital longitude of Ganymede is 40° [*Grodent et al.*, 2008b, Table 1]. This longitude is chosen to be close to the S3 longitude location of the PAD boundary at the time the HST image was taken. Ganymede's footprint is located equatorward of the mapped location of the boundary as it is expected since the boundary is observed at slightly larger distances (17–18.5 R_J) than Ganymede's orbital distance (15 R_J). We note that VIP4 would have mapped the PAD boundary several degrees equatorward from Ganymede's footprint [see *Grodent et al.*, 2008b, Figure 3]. For the southern hemisphere we use the VIP4 magnetic field model, since the accuracy of the model at this region has not been questioned. The red dots on the southern projection in Figure 1 show the mapped location of the PAD boundary, close to the limb, within the region of the EDE. The measured auroral brightness at the magnetically mapped location of the boundary is ~15 kR.

3. Energetic Electron Scattering and Auroral Precipitation

[7] The anisotropic pitch angle distribution provides the required energy for wave generation. We verified whether the measured distribution is sufficient to generate waves by comparing the measured electron flux in the energy range of 15 to 304 keV with the critical limit [*Thorne and Tsurutani*, 1979]. The 15-304 keV energy range covers the energy of the precipitating electrons believed to be responsible for the aurora as it is shown in previous studies [*Gustin et al.*, 2004]. The measured flux is always higher than the critical flux, indicating that the production of waves at this region is possible. Figure 2c shows the presence of whistler mode waves in the region of the PAD boundary at the wave frequencies 55 to 300 Hz. Whistler mode waves can scatter electrons into the loss cone and lead to electron precipitation in the ionosphere. We test whether the conditions for strong pitch angle diffusion are met at the region of the PAD boundary, based on Galileo wave and energetic particle data from which we calculate the ratio of the diffusion coefficient to the strong diffusion limit. The wave measurements during this time interval show high variability. Figure 2d shows the maximum (solid) and minimum (dashed) E and B field power spectra for a given frequency. For the calculation of the diffusion coefficient we take into account the variations in the wave measurements. The pitch angle diffusion coefficient $D_{\alpha\alpha} \sim \frac{2\pi f_c}{\gamma} \cdot \left(\frac{B'}{B}\right)^2 \cdot \epsilon$ [*Thorne and Tsurutani*, 1979] is estimated for the fluctuating resonant wave power B'^2 obtained from the wave measurements for the frequencies 55 to 300 Hz, the measured magnetic field B in the equatorial region of the PAD boundary (40–70 nT), the electron gyrofrequency f_c based on the measured magnetic field, the spectral index $\gamma = 1$ for the non-relativistic electrons and the parameter ϵ for the values 0.1 and 1, which gives the fraction of the electron orbit spent in resonance. We test whether strong diffusion takes place for the electron energy range 15–304 keV of Galileo EPD by comparing the diffusion coefficient $D_{\alpha\alpha}$ with the critical value for strong diffusion $D_{SD} = (\frac{v}{4R_J})1/L^4$ [*Thorne and Tsurutani*, 1979], where L is the radial distance and v the electron's kinetic velocity. We find that the strong diffusion criterion is systematically satisfied for the wave frequencies during which whistler mode waves are observed. Table 1 shows the electron energy ranges and the respective wave frequencies for which strong diffusion takes place. The strong diffusion limit is calculated in a dipolar field approximation. This is reasonable for the PAD boundary region, because it is located at several Jovian radii from the surface, where the higher order components of the magnetic field vanish. Additionally, the diffusion coefficient is well above the strong diffusion limit.

Table 1. Electron Energy Range and the Corresponding Wave Frequencies for Which the Strong Diffusion Limit is Satisfied

Electron Energy Range (keV)	Whistler Mode Wave Frequency (Hz)
15–55	<314
55–93	<250
93–304	<150

[8] Assuming strong diffusion, we calculate the precipitation energy flux ε [*Thorne*, 1983] given by

$$\varepsilon = \pi \int_{E_{min}}^{E_{max}} EJ(E)dE, \quad (1)$$

where the electron flux $J \propto E^{-\gamma}$, E the energy and γ is the spectral index. The energy flux is calculated in the energy range 15 to 304 keV, based on the electron energy spectra measured along the PAD boundary shown in Figure 2d. The energy precipitation flux is found to range between 1.2 and 7.2 mW m^{-2} and supports auroral brightness of 12-72 kR, assuming that 1 mW m^{-2} of injected electrons corresponds to

FUV emission of 10 kR [*Grodent et al.*, 2001]. The derived auroral brightness based on the measurements on the PAD boundary is in accordance with the measured auroral brightness at the ionospheric counterpart of the boundary (50 kR in the North, 15 kR in the South) and at the general EDE region (40–100 kR in the North, 10–40 kR in the South).

4. Conclusions

[9] Based on simultaneous HST and Galileo observations we examine the EDE and their relation to the energetic electron scattering. The PAD boundary magnetically maps to the diffuse auroral emission region in the northern and southern hemisphere. Whistler mode waves observed simultaneously at the same region can scatter electrons into the loss cone and lead to electron precipitation in the ionosphere. Based on wave and energetic electron measurements we estimate the energy flux precipitated in the ionosphere by electron scattering due to whistler mode waves. The comparison of the derived precipitation energy flux with the observed brightness of the EDE shows that the energy contained in the PAD boundary can account for the auroral emissions. Based on the mapped location of the boundary and the derived precipitation energy flux, we suggest that electron scattering by whistler mode waves is contributing to the EDE in both hemispheres.

[10] The persistence of the EDE suggests that its origin is associated with a permanent magnetospheric feature such as the PAD boundary, which is observed at almost all Galileo orbits [*Tomás et al.*, 2004a]. The confinement of the PAD boundary relates it to a narrow belt of auroral emissions. This is supported by the present set of simultaneous observations, especially in the north. The ionospheric location of the boundary is shown to be placed at one of the two quasi-parallel arcs and particularly at the poleward one, as indicated by the magnetic mapping (Figure 1). In the southern hemisphere the mapped location of the boundary close to the limb does not allow us to conclude on the corresponding auroral feature. The rest of the diffuse emissions could be related to other mechanisms, such as electron scattering by whistler mode waves associated with anisotropic injection events [*Xiao et al.*, 2003; *Mauk et al.*, 2002]. Indeed Figure 2 shows evidence of whistler mode excitation at distances $<17\ R_J$ which could magnetically map to the equatorward arc. However, in the present work we do not show additional evidence justifying an association of the auroral emission with the whistler mode variations related to injection events.

[11] **Acknowledgments.** This work is based on observations with the NASA/ESA Hubble Space Telescope, obtained at the Space Telescope Science Institute (STScI), which is operated by AURA, inc. for NASA under contract NAS5-26555. The research was supported by the Belgian Fund for Scientific Research (FNRS) and the PRODEX Program managed by the European Space Agency in collaboration with the Belgian Federal Science Policy Office. The authors thank Andreas Lagg for providing the EPD software.

References

Bhattacharya, B., R. M. Thorne, and D. J. Williams (2001), On the energy source for diffuse Jovian auroral emissivity, *Geophys. Res. Lett.*, *28*, 2751–2754.

Bhattacharya, B., R. M. Thorne, D. J. Williams, K. K. Khurana, and D. A. Gurnett (2005), Diffuse auroral precipitation in the Jovian upper atmosphere and magnetospheric electron flux variability, *Icarus*, *178*, 406–416.

Clarke, J. T., et al. (1998), Hubble Space Telescope imaging of Jupiter's UV aurora during the Galileo orbiter mission, *J. Geophys. Res.*, *103*, 20,217–20,236.

Connerney, J. E. P., M. H. Acuña, N. F. Ness, and T. Satoh (1998), New models of Jupiter's magnetic field constrained by the Io flux tube footprint, *J. Geophys. Res.*, *103*, 11,929–11,939.

Cowley, S. W. H., and E. J. Bunce (2001), Origin of the main auroral oval in Jupiter's coupled magnetosphere-ionosphere system, *Planet. Space Sci.*, *49*, 1067–1088.

Grodent, D., J. H. Waite Jr., and J.-C. Gérard (2001), A self-consistent model of the Jovian auroral thermal structure, *J. Geophys. Res.*, *106*, 12,933–12,952.

Grodent, D., J. T. Clarke, J. Kim, J. H. Waite Jr., and S. W. H. Cowley (2003a), Jupiter's main auroral oval observed with HST-STIS, *J. Geophys. Res.*, *108*(A11), 1389, doi:10.1029/2003JA009921.

Grodent, D., J. T. Clarke, J. H. Waite Jr., S. W. H. Cowley, J.-C. Gérard, and J. Kim (2003b), Jupiter's polar auroral emissions, *J. Geophys. Res.*, *108*(A10), 1366, doi:10.1029/2003JA010017.

Grodent, D., J.-C. Gérard, A. Radioti, B. Bonfond, and A. Saglam (2008a), Jupiter's changing auroral location, *J. Geophys. Res.*, *113*, A01206, doi:10.1029/2007JA012601.

Grodent, D., B. Bonfond, J.-C. Gérard, A. Radioti, J. Gustin, J. T. Clarke, J. Nichols, and J. E. P. Connerney (2008b), Auroral evidence of a localized magnetic anomaly in Jupiter's northern hemisphere, *J. Geophys. Res.*, *113*, A09201, doi:10.1029/2008JA013185.

Gustin, J., J.-C. Gérard, D. Grodent, S. W. H. Cowley, J. T. Clarke, and A. Grard (2004), Energy-flux relationship in the FUV Jovian aurora deduced from HST-STIS spectral observations, *J. Geophys. Res.*, *109*, A10205, doi:10.1029/2003JA010365.

Horne, R. B., R. M. Thorne, N. P. Meredith, and R. R. Anderson (2003), Diffuse auroral electron scattering by electron cyclotron harmonic and whistler mode waves during an isolated substorm, *J. Geophys. Res.*, *108*(A7), 1290, doi:10.1029/2002JA009736.

Mauk, B. H., J. T. Clarke, D. Grodent, J. H. Waite Jr., C. P. Paranicas, and D. J. Williams (2002), Transient aurora on Jupiter from injections of magnetospheric electrons, *Nature*, *415*, 1003–1005.

Radioti, A., J.-C. Gérard, D. Grodent, B. Bonfond, N. Krupp, and J. Woch (2008), Discontinuity in Jupiter's main auroral oval, *J. Geophys. Res.*, *113*, A01215, doi:10.1029/2007JA012610.

Thorne, R. M. (1983), Microscopic plasma processes in the Jovian magnetosphere, in *Physics of the Jovian Magnetosphere*, edited by A. J. Dessler, pp. 454–488, Cambridge Univ. Press, New York.

Thorne, R. M., and B. T. Tsurutani (1979), Diffuse Jovian aurora influenced by plasma injection from Io, *Geophys. Res. Lett.*, *6*, 649–652.

Tomás, A. T., J. Woch, N. Krupp, A. Lagg, K.-H. Glassmeier, M. K. Dougherty, and P. G. Hanlon (2004a), Changes of the energetic particles characteristics in the inner part of the Jovian magnetosphere: A topological study, *Planet. Space Sci.*, *52*, 491–498.

Tomás, A. T., J. Woch, N. Krupp, A. Lagg, K.-H. Glassmeier, and W. S. Kurth (2004b), Energetic electrons in the inner part of the Jovian magnetosphere and their relation to auroral emissions, *J. Geophys. Res.*, *109*, A06203, doi:10.1029/2004JA010405.

Xiao, F., R. M. Thorne, D. A. Gurnett, and D. J. Williams (2003), Whistler-mode excitation and electron scattering during an interchange event near Io, *Geophys. Res. Lett.*, *30*(14), 1749, doi:10.1029/2003GL017123.

B. Bonford, J.-C. Gérard, D. Grodent, J. Gustin, and A. Radioti, Laboratoire de Physique Atmosphérique et Planétaire, Institut d'Astrophysique et de Géophysique, Université de Liège, Allee du 6 Aout, 17, B-4000 Liège, Belgium. (a.radioti@ulg.ac.be)

N. Krupp and J. Woch, Max-Planck-Institut für Sonnensystemforschung, Max-Planck-Std. 2, D-37191 Katlenburg-Lindau, Germany.

J. D. Menietti, Department of Physics and Astronomy, University of Iowa, 203 Van Allen Hall, Iowa City, IA 52242-1479, USA.

A. T. Tomás, GeoForschungsZentrum, Telegrafenberg, D-14473 Potsdam, Germany.